Carbohydrate Polymers 81 (2010) 49–56

Contents lists available at ScienceDirect

Carbohydrate Polymers

journal homepage: www.elsevier.com/locate/carbpol

Chitosan oligosaccharides inhibit TNF-α-induced VCAM-1 and ICAM-1 expression in human umbilical vein endothelial cells by blocking p38 and ERK1/2 signaling pathways

Hong-Tao Liu [a,b,c], Wen-Ming Li [b], Pei Huang [b], Wen-Juan Chen [b], Qi-Shun Liu [a], Xue-Fang Bai [a], Chao Yu [b,*], Yu-Guang Du [a,*]

[a] Laboratory of Natural Products and Glyco-engineering Research, Dalian Institute of Chemical Physics, Chinese Academy of Sciences, 457, Zhong-shan Road, Dalian 116023, China
[b] Institute of Life Sciences, Chongqing Medical University, Chongqing 400016, China
[c] The Graduate School of Chinese Academy of Sciences, Beijing 110864, China

ARTICLE INFO

Article history:
Received 15 July 2009
Received in revised form 19 November 2009
Accepted 25 January 2010
Available online 1 February 2010

Keywords:
Chitosan oligosaccharides
Vascular cell adhesion molecule-1
Intercellular adhesion molecule-1
Tumor necrosis factor-α
Mitogen-activated protein kinases
Human umbilical vein endothelial cells

ABSTRACT

This study aimed to investigate the inhibitive effects of chitosan oligosaccharides (COS) on tumor necrosis factor (TNF)-α-induced over-expression of vascular adhesion molecule-1 (VCAM-1) and intercellular adhesion molecule-1 (ICAM-1) in human umbilical vein endothelial cells (HUVECs). We found that COS effectively inhibited TNF-α-induced expression of VCAM-1 and ICAM-1 at the level of transcription and translation. Signal transduction studies suggested that COS blocked TNF-α-induced activation of NF-κB, degradation of IκBα, and phosphorylation of p38 MAPK and ERK1/2. A further investigation showed that the NF-κB activation can be partly suppressed by p38 MAPK inhibitor (SB203580) and ERK1/2 inhibitor (PD98059), which also ameliorated the mRNA expression of VCAM-1 and ICAM-1 in TNF-α-induced HUVECs. Additionally, COS decreased U937 monocyte adhesion to HUVECs induced by TNF-α. Our findings suggest that COS inhibit VCAM-1 and ICAM-1 production in activated HUVECs at least partly through the blockade of p38 and ERK1/2 signaling pathways.

1. Introduction

Tumor necrosis factor (TNF)-α, a member of TNF ligand family, is one of the major inflammatory cytokines and mediates systemic inflammation by interaction with its receptors expressed on different cells (Nizamutdinova et al., 2007). Among these cells, vascular endothelium is shown to be a main action site of TNF-α. It has been confirmed that the induction of endothelial cells by TNF-α leads to activation of multiple signal transduction pathways and subsequently initiates the over-expression of related pro-inflammatory cytokines such as adhesion molecules, interleukins and monocyte-chemoattractant protein-1 (Haubner et al., 2007; Vietor, Schwenger, Li, Schlessinger, & Vilcek, 1993).

Vascular cell adhesion molecule-1 (VCAM-1) and intercellular adhesion molecule-1 (ICAM-1), the members of immunoglobulin superfamily, are predominantly expressed on the surface of endothelial cells and smooth muscle cells (Kim et al., 2008; Winterbone, Tribolo, Needs, Kroon, & Hughes, 2009). Both adhesion molecules are expression products of highly inducible genes and play important roles in local inflammatory responses occurring in vascular walls (Séguin et al., 2008). At early stages of vascular inflammation, endothelial cells will elicit the up-regulation of VCAM-1 and ICAM-1 levels, which mediate the leukocyte adhesion to activated endothelial cells and ultimately promote the progression of endothelial dysfunction (Kim et al., 2008). Therefore, therapeutic agents with suppressive effects on adhesion molecules might have potential application in treatment of vascular disorders.

Chitin, the polymer of D-glucosamine in β (1,4) linkage, is the major component of exoskeleton of crustaceans and cell wall of fungi (Pae et al., 2001). Chitosan is deacetylated products of chitin. Chitosan oligosaccharides (COS) are degraded products of chitosan, or the deacetylated and degraded products of chitin by chemical and enzymatic hydrolysis. So far, COS have been widely used as healthy foods in several countries for their versatile bioactivities. It was reported that COS possessed protective effects on glycerol-induced acute renal failure in rats and carbon tetrachloride-induced liver toxicity in mice (Yan, Wanshun, Baoqin, Bing, & Chenwei, 2006; Yoon et al., 2008). COS were also shown to act as antioxidants that effectively scavenge free radicals in either cellular oxidizing systems or cell-free assay systems (Je, Park, & Kim, 2004; Mendis, Kim, Rajapakse, & Kim, 2007). In addition, COS were confirmed to have antibacterial,

* Corresponding authors. Tel.: +86 411 84379061; fax: +86 411 84379060.
E-mail addresses: yuchaom@163.com (C. Yu), articles1805@gmail.com (Y.-G. Du).

0144-8617/$ - see front matter © 2010 Elsevier Ltd. All rights reserved.
doi:10.1016/j.carbpol.2010.01.054

antitumor, and immunopotentiating activities (Moon et al., 2007; Pae et al., 2001). Recent studies have additionally demonstrated that COS display anti-inflammatory properties in immunocytes including the inhibition of nitric oxide, the down-regulation of interleukin-6 and TNF-α, and the increase of cell viability of neutrophils (Dou et al., 2007; Wu & Tsai, 2007; Yoon, Moon, Park, Im, & Kim, 2007). Noticeably, although much information has been gained regarding the pronounced bioactivities of COS in pharmaceutical and medical fields, relatively little is known about the roles for COS in vascular inflammation.

The principle objective of this study was to determine whether COS could inhibit TNF-α-induced VCAM-1 and ICAM-1 production in human umbilical vein endothelial cells (HUVECs), which were commonly accepted as a tool in investigating the pathogenesis of endothelial damage (Lidington, Moyes, McCormack, & Rose, 1999). We evaluated the inhibitory effects of COS on TNF-α-induced VCAM-1 and ICAM-1 expression in HUVECs, as well as the adhesion of U937 monocytes to activated HUVECs. Secondly, to determine the underlying intracellular mechanism of suppressive effects of COS, the roles of nuclear factor κB (NF-κB), inhibitory factor κB-α (IκBα) and mitogen-activated protein kinases (MAPKs) in HUVECs after TNF-α challenge were explored.

2. Materials and methods

2.1. Chemicals and reagents

COS were prepared by our laboratory (the degree of deacetylation was above 95%) (Zhang, Du, Yu, Mitsutomi, & Aiba, 1999). The weight percentages of COS with DP (degree of polymerization) 2–6 in oligo-mixture were 3.7%, 16.1%, 28.8%, 37.2%, and 14.2%, respectively. Recombinant human TNF-α was obtained from Prospec-Tany Technogene Ltd. (Rehovot, Israel) and 3-(4,5-dimethylthiazol-2-yl)-2,5-diphenyltetrazolium bromide (MTT) from Sigma (St. Louis, MO, USA). ERK1/2 inhibitor (PD98059) and p38 MAPK inhibitor (SB203580) were purchased from Invitrogen Corporation (Carlsbad, CA, USA). Horseradish peroxidase (HRP)-conjugated goat anti-rabbit IgG, rabbit anti-nuclear factor κB (NF-κB) p65 polyclonal antibody and 2′,7′-bis-(2-carboxyethyl)-5-(and-d)-carboxyfluorescein, acetoxymethyl ester (BCECF-AM) were obtained from Beyotime Institute of Biotechnology (Jiangsu, China). Rabbit anti-VCAM-1 and anti-ICAM-1 were purchased from America Basic Gene Associate Bioscience, Inc (Chicago, USA). Rabbit anti-IκBα, anti-p38 MAPK, anti-phospho-p38 (p-p38) MAPK, anti-ERK1/2, anti-phospho-ERK1/2 (p-ERK1/2) and anti-GAPDH polyclonal antibody were obtained from Santa Cruz Biotechnology (CA, USA). Dulbecco's-modified Eagle's medium F12 (DMEM-F12), RPMI-1640 medium and fetal bovine serum (FBS) were purchased from Gibco (Grand Island, NY, USA).

2.2. Cell culture and drug treatment

HUVECs were isolated from normal human umbilical cords, digested with 0.05% trypsin containing 0.02% EDTA, and eluted with DMEM-F12. Isolated HUVECs were cultured in DMEM-F12 supplemented with 10% FBS, 100 U/ml penicillin, 100 U/ml streptomycin, 30 μg/ml endothelial cell growth supplements, and 5 U/ml heparin at 37 °C under 5% CO_2 and 95% air. Passage 2–6 was used for experiments. The U937 monocyte, bought from Wuhan Institute of Cell Biology (Wuhan, China), was cultured in RMPI-1640 medium containing 10% FBS and antibiotics. For most experiments, HUVECs reaching sub-confluence were pre-incubated with vehicle or COS in DMEM-F12 with 1% FBS for 24 h. After pre-incubation, cells were induced with TNF-α in the absence of COS for indicated time and then subjected to further analysis.

2.3. Cell viability assay

Cell viability was evaluated by MTT analysis, which relies upon the cellular reduction of positively charged tetrazolium salts to their intensely colored formazan product by mitochondrial dehydrogenases (Cianchetti et al., 2008). In short, HUVECs were plated at a density of 5×10^3 cells/well into 96-well culture plates and grown to sub-confluence. Next, cells were incubated with different concentrations of COS (50–200 μg/ml) in 1% FBS-containing DMEM-F12 for 24 h. After that, cells were washed with phosphate-buffered saline (PBS, pH 7.4) twice and followed by the incubation with 100 μl of MTT solubilization solution (5 mg/ml) in culture medium at 37 °C for another 3 h. After MTT removal, the colored formazan was dissolved in 100 μl of dimethylsulfoxide (DMSO). Absorbance was measured by spectrophotometry at 490 nm using a Sunrise Remote Microplate Reader (Grodlg, Austria). The cell viability in each well was presented as percentage of control cells.

2.4. RNA isolation and reverse transcription-polymerase chain reaction (RT-PCR) analysis

Total cellular RNA was extracted from HUVECs using the TRIZOL reagent (Takara, Dalian, China) and the concentration of RNA isolates was determined spectrophotometrically using a DNA/RNA Gene-Quant Calculator (Amersham Biosciences, USA). The expression level of mRNA was examined by RT-PCR analysis (Bioer, Hangzhou, China) using an Eppendorf 5332 thermocycler (Eppendorf AG, Germany). The sequences of sense and antisense primers for VCAM-1 (720 bp) were 5′-GCA AGG TTC CTA GCG TGT A-3′ and 5′-CTC CCG CAT CCT TCA ACT-3′, respectively. The ICAM-1 primers (289 bp) were (sense) 5′-CGA CTG GAC GAG AGG GAT TG-3′ and (antisense) 5′- TTA TGA CTG CGG CTG CTA CC-3′. The GAPDH primers (230 bp) were (sense) 5′-CTC TCT GCT CCT CCT GTT CGA CAG-3′ and (antisense) 5′-GTG GAA TCA TAT TGG AAC ATG T-3′. Total RNA was reverse-transcribed into cDNA with random primers and AMV reverse transcriptase at 42 °C for 60 min. The following conditions were used for PCR amplification: 4 min at 94 °C for the initial denaturation; 30 cycles × 30 s at 94 °C, 45 s at 54 °C, and 45 s at 72 °C for VCAM-1; 25 cycles × 30 s at 94 °C, 30 s at 55 °C, and 30 s at 72 °C for ICAM-1; 30 cycles × 30 s at 94 °C, 30 s at 54 °C, and 30 s at 72 °C for GAPDH. The PCR product from each sample was electrophoresed on a 2% agarose gel containing 1% GoldView™. Gels were visualized and photographed by a Chemi-Doc image analyzer (Bio-Rad, Hercules, CA, USA). Quantitative data normalized to GAPDH were obtained using the ImageJ system software (NIH, USA).

2.5. Preparation of cell lysates

Preparation of cytoplasmic and nuclear fraction was performed by using nuclear and cytoplasmic protein extraction kit according to the manufacturer's instructions (Beyotime, Jiangsu, China). Briefly, cells were washed twice with ice-cold PBS (pH 7.4), detached and suspended in 200 μl of lysis buffer A (10 mM Hepes with pH 7.9, 10 mM KCl, 0.1 mM EDTA, 1 mM dithiothreitol, 0.4% Igepal CA-630, 5 μM leupeptin, 2 μM pepstatin A, 1 μM aprotinin, and 1 mM phenylmethylsulfonyl fluoride) for 10 min. The cell lysates were subjected to centrifugation at 12,000*g* for 5 min and the supernatant was aliquoted for cytoplasmic proteins. The pellets were washed once with 200 μl of buffer A and resuspended in 50 μl of nuclear extraction buffer B (20 mM Hepes with pH 7.9, 0.4 M NaCl, 1 mM EDTA, 1 mM dithiothreitol, and 1 mM phenylmethylsulfonyl fluoride). The suspension was agitated for 30 min at 4 °C and centrifuged at 12,000*g* for 10 min. The supernatant fraction containing nuclear proteins was collected. For isolation of total cell extracts, cells were lysed in RIPA lysis buffer (50 mM Tris with

pH 7.4, 150 mM NaCl, 1% Triton X-100, 1% sodium deoxycholate, 0.1% SDS, and 0.05 mM EDTA). After being kept on ice for 15 min, the lysates were centrifuged at 12,000*g* for 10 min. Protein concentration was determined by using the bicinchoninic acid protein assay kit (BioMed, Beijing, China). All samples were stocked at −80 °C for further analysis.

2.6. Western blot analysis

For Western blot analysis, an aliquot of protein samples from cell lysates was diluted with 5× SDS sample buffer (1 M Tris–HCl, 8% dithiothreitol, 10% SDS, 50% glycerol, and 0.5% bromophenol blue), and the samples were boiled for 10 min. Next, 50 μg of protein were subjected to 6–12% SDS–polyacrylamide gel electrophoresis at 100 V. The separated proteins were transferred to 0.45 μm polyvinylidene fluoride membranes for 90 min at 250 mA. The membranes were blocked with 5% skim milk in PBS containing 0.1% Tween 20 (PBST) for 1 h at room temperature. After that, the membranes were incubated with anti-VCAM-1, anti-ICAM-1, anti-NF-κB (p65), anti-IκBα, anti-p38, anti-p-p38, anti-ERK1/2, anti-p-ERK1/2, and anti-GAPDH in 5% skim milk in PBST overnight at 4 °C, and the bound antibody was detected by HRP-conjugated anti-rabbit IgG for 1 h. The membranes were washed and developed using enhanced chemiluminescence reagents and the densitometric analysis was performed with the use of PDI Imageware System (Bio-Rad, Hercules, CA, USA).

2.7. Monocyte adhesion assay

The monocyte adhesion assay was performed as previously described (Zhou, Liu, Miao, & Wang, 2005). In brief, HUVECs were seeded in 24-well culture plates at 5×10^4 cells/well for 48 h before experiments. U937 monocytes were labeled with the fluorescent dye BCECF-AM at 10 μM final concentration in RPMI-1640 medium containing 10% FBS at 37 °C for 1 h. The labeled cells were then harvested by centrifugation, washed three times with PBS, and resuspended in the medium. Subsequently, labeled cells were added to HUVECs in 24-well culture plates at 5×10^4 cells/well and incubated at 37 °C for 1 h. After the co-incubation, cell suspensions were withdrawn and HUVECs were gently washed with PBS. Fluorescent images were obtained using a Leica DMRX microscope (Wetzlar, Germany), and fluorescent intensity of each sample was measured with the Image-Pro Plus 6.0 software (Media Cybernetics, USA).

2.8. Statistics

Statistical analyses were performed by using the SPSS 10.0 package (SPSS Inc., Chicago, IL, USA). All data were presented as means ± *SD* of three to five independent experiments. The differences among groups were analyzed by One-way ANOVA and Student's *t*-test. Values of $P < .05$ were considered to be statistically significant.

3. Results

3.1. Time–response studies of VCAM-1 and ICAM-1 mRNA expression in TNF-α-induced HUVECs

We first carried out the time–response studies of VCAM-1 and ICAM-1 mRNA expression in TNF-α-induced HUVECs by RT-PCR analysis. As shown in Fig. 1A, after treatment with TNF-α (20 ng/ml) for the time indicated, mRNA expression levels of both VCAM-1 and ICAM-1 were significantly increased as compared to the vehicle-treated group ($P < .05$). The magnitude of mRNA up-regulation for VCAM-1 and ICAM-1 peaked at 6 h after TNF-α exposure (5.6- and 4.2-fold of control, respectively, $P < .01$). Based on theses results, HUVECs were treated with vehicle or 20 ng of TNF-α for 6 h in the extensive studies.

3.2. Inhibitory effects of COS on VCAM-1 and ICAM-1 mRNA expression in TNF-α-induced HUVECs

To determine the inhibitory effects of COS on VCAM-1 and ICAM-1 mRNA expression in TNF-α-induced HUVECs, cells were pretreated with various concentrations of COS (50–200 μg/ml) for 24 h and then exposed to TNF-α (20 ng/ml) for 6 h. The VCAM-1 and ICAM-1 mRNA expression levels were evaluated by

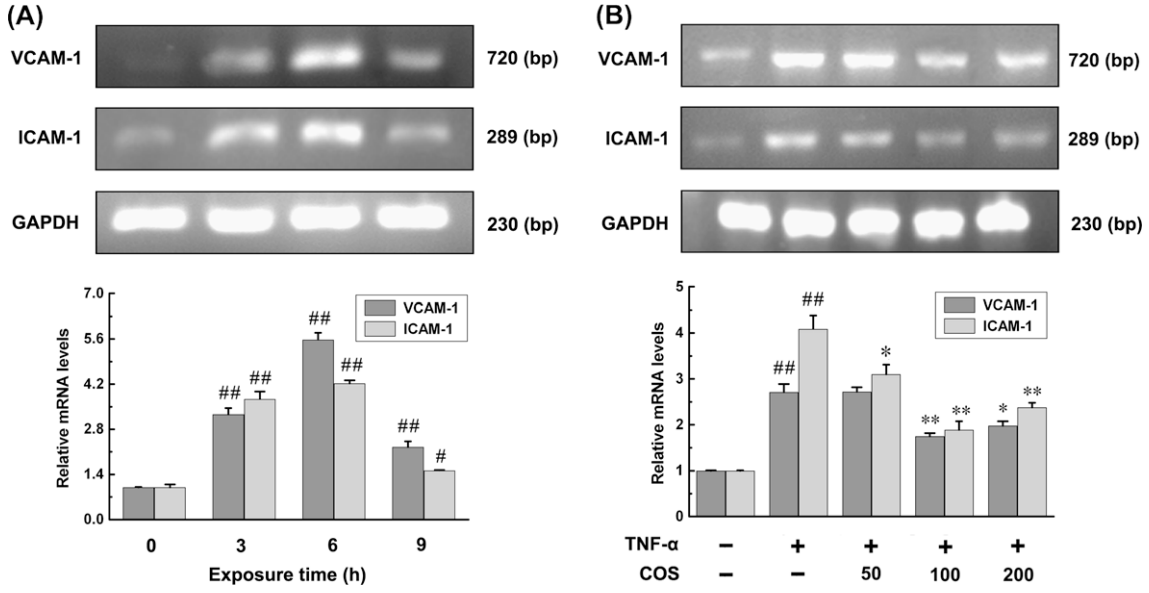

Fig. 1. TNF-α induces VCAM-1 and ICAM-1 mRNA expression in HUVECs (A), and COS inhibit VCAM-1 and ICAM-1 mRNA expression in TNF-α-induced HUVECs (B). Cells were induced by TNF-α (20 ng/ml) for different intervals (A) or pretreated with COS (50, 100, and 200 μg/ml) for 24 h before exposure to TNF-α for 6 h (B). Data are representative of three experiments (means ± *SD*). $^{\#\#}P < .01$ compared to the vehicle-treated group; $^{*}P < .05$, $^{**}P < .01$ compared to the TNF-α-treated group.

RT-PCR analysis. As illustrated in Fig. 1B, both adhesion molecules were up-regulated by TNF-α but were markedly inhibited by pretreatment with COS. The maximal inhibitory effects of COS were obtained at 100 μg/ml and the mRNA expression levels of VCAM-1 and ICAM-1 were separately decreased to 64.7% and 46.1% of the TNF-α-treated group ($P < .01$). Furthermore, this inhibition was not due to the cytotoxicity of COS because that no difference was observed in cell viability between cells treated with COS alone and controls as determined by MTT assay (data not shown).These results indicate that COS interfere with TNF-α-induced VCAM-1 and ICAM-1 expression at the transcriptional level.

3.3. Inhibitory effects of COS on VCAM-1 and ICAM-1 protein expression in TNF-α-induced HUVECs

We next examined the inhibition of COS on VCAM-1 and ICAM-1 protein levels by Western blot analysis. The results in Fig. 2 show that, HUVECs constitutively expressed low levels of VCAM-1 and ICAM-1 protein, which were drastically increased by TNF-α (20 ng/ml) challenge for 6 h (1.8- and 3.4-fold of the vehicle-treated group, respectively, $P < .01$). Nonetheless, the pretreatment with COS (50–200 μg/ml) for 24 h before TNF-α exposure caused a marked decrease in VCAM-1 and ICAM-1 protein levels, both of which were completely suppressed by COS at the concentration of 100 μg/ml (33.3% and 15.6% of the TNF-α-treated group, respectively, $P < .01$).

3.4. Effects of COS on TNF-α-induced NF-κB activation and IκBα degradation in HUVECs

NF-κB, localized in the cytoplasm, can be activated by TNF-α and translocates into the nucleus to promote gene transcription of pro-inflammatory cytokines (Nizamutdinova et al., 2007). To investigate the inhibitory effects of COS on TNF-α-induced NF-κB activation in HUVECs, NF-κB expression in both cytoplasmic and nucleic fractions was determined. As shown in Fig. 3A, after TNF-α (20 ng/ml) challenge alone for 6 h, NF-κB p65 proteins showed an explosive increase (17.2-fold of the vehicle-treated group, $P < .01$) in the nucleus and a pronounced decrease in the cytoplasm (42.3% of the vehicle-treated group, $P < .01$). By contrast, the pretreatment with COS (50, 100, and 200 μg/ml) for 24 h before TNF-α exposure led to a striking down-regulation of nuclear NF-κB p65 proteins (23.2%, 9.2%, and 29.6% of the TNF-α-treated group, respectively, $P < .01$) and a remarkable up-regulation of cytoplasmic NF-κB p65 protein (5.5-, 9.4-, and 1.8-fold of the TNF-α-treated group, respectively, $P < .01$), which suggests that COS effectively inhibited the TNF-α-induced NF-κB activation in HUVECs.

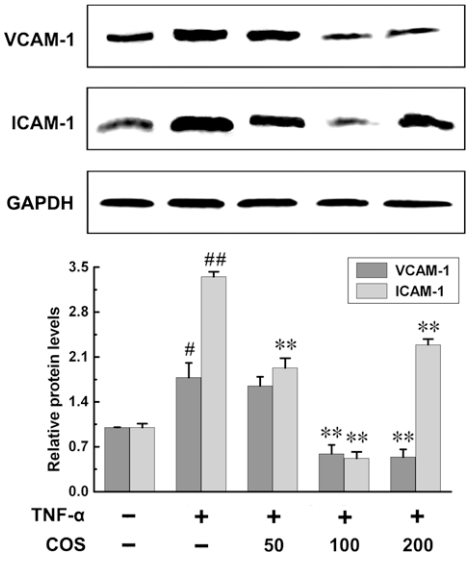

Fig. 2. COS inhibit VCAM-1 and ICAM-1 production in TNF-α-induced HUVECs. Cells were pretreated with COS (50, 100, and 200 μg/ml) for 24 h and then exposed to TNF-α (20 ng/ml) for 6 h. Data are representative of three experiments (means ± *SD*). $^{\#}P < .05$, $^{\#\#}P < .01$ compared to the vehicle-treated group; $^{**}P < .01$ compared to the TNF-α-treated group.

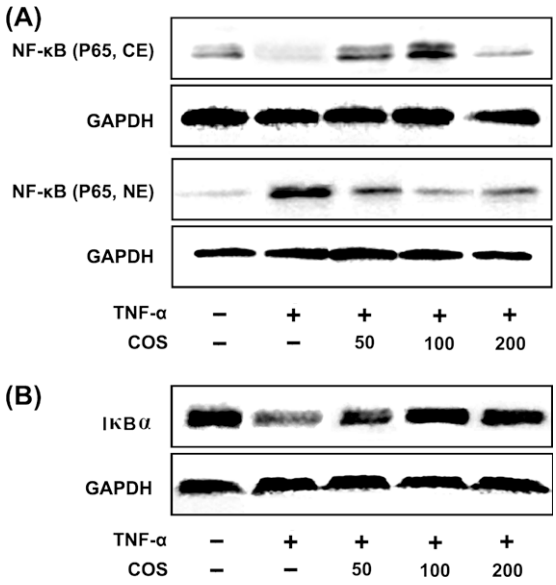

Fig. 3. COS inhibit TNF-α-induced NF-κB activation (A) and IκBα degradation (B) in HUVECs. NE, nuclear extracts; CE, cytoplasmic extracts. (A) Cells were pretreated with COS (50, 100, and 200 μg/ml) for 24 h and then exposed to TNF-α (20 ng/ml) for 6 h. (B) Cells were pretreated with COS (50, 100, and 200 μg/ml) for 24 h and then exposed to TNF-α (20 ng/ml) for 1 h. Data are representative of three experiments (means ± *SD*).

IκBα, an inhibitor of NF-κB activation, can be degraded by TNF-α to initiate the NF-κB translocation into nucleus (Sun et al., 2008). Therefore, the suppressive effects of COS on TNF-α-induced IκBα degradation were also determined. As shown in Fig. 3B, the TNF-α (20 ng/ml) exposure to HUVECs for 1 h resulted in a marked degradation of IκBα (24% of the vehicle-treated group, $P < .01$), which was obviously suppressed by the pretreatment with COS (50, 100, and 200 μg/ml) for 24 h before TNF-α exposure (1.6-, 5.6-, and 3.1-fold of the TNF-α-treated group, respectively, $P < .05$ or .01).

3.5. Effects of COS on p38 MAPK and ERK1/2 pathways in TNF-α-induced HUVECs

To evaluate potential roles of MAPK pathways in TNF-α-induced HUVECs, we treated the cells with TNF-α (20 ng/ml) for different time intervals and observed that TNF-α rapidly increased the levels of p-p38 MAPK and p-ERK1/2 with similar potency and efficacy (Fig. 4A). The maximal phosphorylation of both MAPKs was observed at 30 min (4.6- and 3.8-fold of the vehicle-treated group, respectively, $P < .01$) and then began to decline at 60 min after TNF-α challenge.

Base on the above results, we examined effects of COS on p-p38 and p-ERK1/2 levels in HUVECs induced by TNF-α (20 ng/ml) for 30 min. As shown in Fig. 4B, TNF-α-induced phosphorylation of p38 MAPK in HUVECs was considerably suppressed by the pretreatment with COS (50–200 μg/ml) for 24 h. In particular, COS from 100 to 200 μg/ml exhibited an entire suppression on p38 phosphorylation ($P < .01$). Also, COS inhibited the level of p-ERK1/

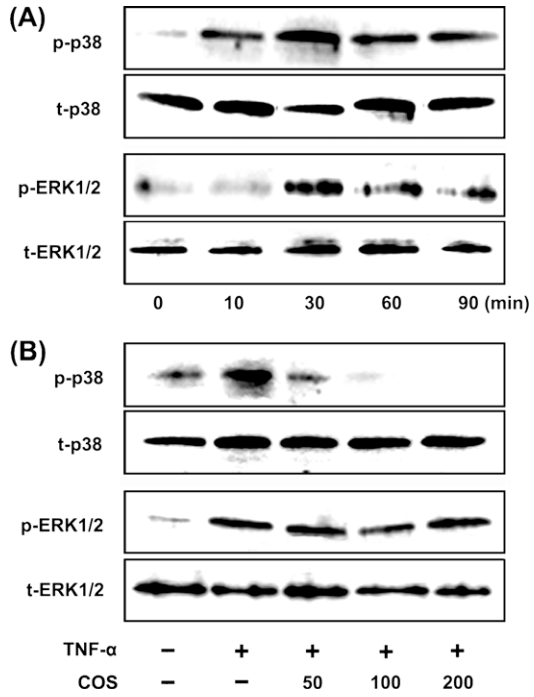

Fig. 4. TNF-α induces the activation of p38 MAPK and ERK1/2 in a time-dependent manner (A), and COS inhibit the phosphorylation of p38 MAPK and ERK1/2 in HUVECs (B). (A) Cells were treated with TNF-α (20 ng/ml) for different time intervals (0–90 min). (B) Cells were pretreated with COS (50–200 μg/ml) for 24 h before exposure to TNF-α (20 ng/ml) for 30 min. Data are representative of three experiments (means ± *SD*).

2 with similar potency but less efficaciously, and the maximal inhibition was at 100 μg/ml (68.1% of the TNF-α-treated group, $P < .01$). In addition, the treatment of HUVECs with COS (50–200 μg/ml) alone failed to change the total and phosphorylated protein levels of both MAPKs (data not shown).

3.6. Roles of p38 MAPK and ERK1/2 in TNF-α-induced NF-κB activation in HUVECs

To confirm whether p38 MAPK and ERK1/2 are involved in the NF-κB activation in TNF-α-induced HUVECs, we tested the effects of p38 MAPK inhibitor, SB203580, and ERK1/2 inhibitor, PD98059, on TNF-α-induced NF-κB translocation into the nucleus. Fig. 5 shows that, TNF-α (20 ng/ml) challenge for 6 h triggered an enhanced NF-κB protein level of nuclear extracts in HUVECs by Western blot analysis, in accordance with previous experiments. On the contrary, pretreatment of HUVECs with SB203580 (25 μM) or PD98059 (30 μM) for 1 h before TNF-α exposure displayed predominant inhibitory effects on the up-regulated NF-κB level by TNF-α (30.4% and 5.7% of the TNF-α-induced group, respectively, $P < .01$).

3.7. Roles of p38 MAPK and ERK1/2 in TNF-α-induced VCAM-1 and ICAM-1 mRNA expression in HUVECs

To further investigate the roles of MAPKs in TNF-α-induced VCAM-1 and ICAM-1 production in HUVECs, cells were pretreated with p38 MAPK inhibitor, SB203580 (25 μM), and ERK1/2 inhibitor, PD98059 (30 μM), for 1 h and then exposed to TNF-α (20 ng/ml) for 6 h. As revealed in Fig. 6, inhibiting p38 MAPK and ERK1/2 with the specific inhibitor SB203580 and PD98059 markedly reduced the mRNA levels of VCAM-1 and ICAM-1 when compared to cells treated with TNF-α alone. In comparison with the TNF-α-treated

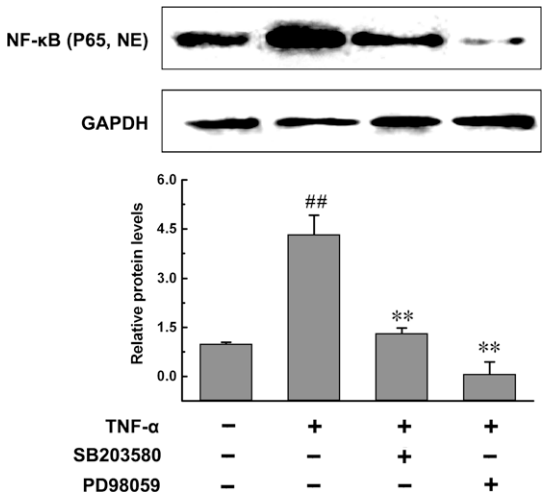

Fig. 5. P38 MAPK inhibitor, SB203580 and ERK1/2 inhibitor, PD98059, inhibit TNF-α-induced NF-κB activation in HUVECs. Cells were pretreated with SB203580 (25 μM) or PD98059 (30 μM) for 1 h and then exposed to TNF-α (20 ng/ml) for 6 h. Data are representative of three experiments (means ± *SD*). $^{\#\#}P < .01$ compared to the vehicle-treated group; $^{**}P < .01$ compared to the TNF-α-treated group.

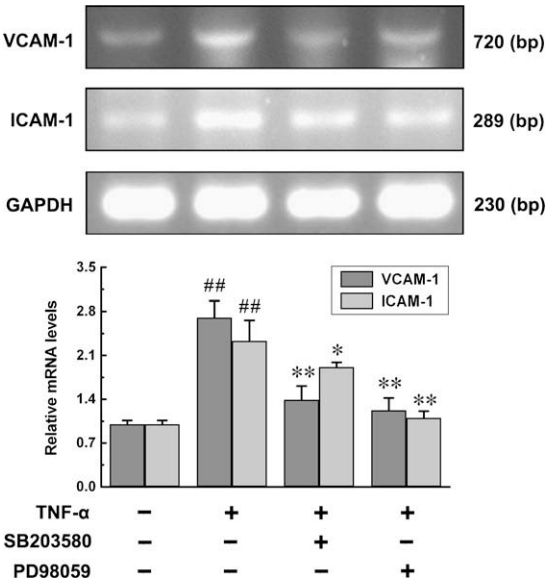

Fig. 6. P38 MAPK inhibitor, SB203580 and ERK1/2 inhibitor, PD98059 inhibit VCAM-1 and ICAM-1 mRNA expression in TNF-α-induced HUVECs. Cells were pretreated with SB203580 (25 μM) or PD98059 (30 μM) for 1 h and then exposed to TNF-α (20 ng/ml) for 6 h. Data are representative of three experiments (means ± *SD*). $^{\#\#}P < .01$ compared to the vehicle-treated group; $^{*}P < .05$, $^{**}P < .01$ compared to the TNF-α-treated group.

group, the mRNA expression levels of VCAM-1 and ICAM-1 were separately decreased to 51.5% and 45.3% by SB203580 pretreatment ($P < .01$), and 81.6% and 46.9% ($P < .05$ or .01) by PD98059 pretreatment. Together, these results clearly indicate that p38 MAPK and ERK1/2 play a central role in VCAM-1 and ICAM-1 singling pathways in TNF-α-induced HUVECs.

3.8. Effects of COS on monocyte adhesion to TNF-α-induced HUVECs

TNF-α can modulate leukocyte adhesion and transmigration in vascular inflammatory diseases (Nizamutdinova et al., 2008), and we thus evaluated effects of COS on the binding of U937 cells to TNF-α-induced HUVECs. We found that adhesion of U937 cells to

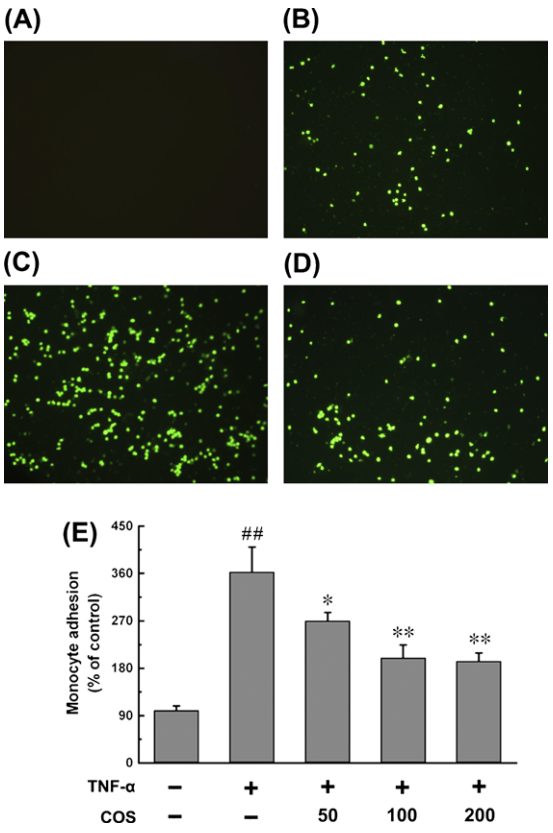

Fig. 7. COS inhibit the binding of U937 monocytes to HUVECs. (A) Immunofluorescent staining of the basal level. (B) Adhesion of fluorescent-labeled U937 cells to vehicle-treated HUVECs. (C) Adhesion of fluorescent-labeled U937 cells to HUVECs induced by TNF-α alone for 6 h. (D) Adhesion of fluorescent-labeled U937 cells to HUVECs pretreated with COS (200 μg/ml) for 24 h before TNF-α exposure for 6 h. (E) Fluorescent intensities of HUVECs treated with vehicle, COS and/or TNF-α. Cells were pretreated with COS (50–200 μg/ml) for 24 h, exposed to TNF-α (20 ng/ml) for 6 h, and then co-incubated with fluorescent-labeled U937 cells for 1 h. Data are expressed as means ± *SD*. ($n = 3$). $^{\#\#}P < .01$ compared to the vehicle-treated group; $^{*}P < .05$, $^{**}P < .01$ compared to the TNF-α-treated group.

HUVECs was increased to 3.6-fold of the control level after TNF-α (20 ng/ml) challenge for 6 h (Fig. 7). Contrary to this, cells pretreated with COS (50–200 μg/ml) for 24 h before TNF-α exposure showed evident reduction of adherent cells to HUVECs from 74.3% to 53.3% of the TNF-α-treated group ($P < .05$ or .01), indicating an effective inhibition of COS on the adhesion of monocytes to TNF-α-induced HUVECs.

4. Discussion

VCAM-1 and ICAM-1 play important roles in the initiation of vascular inflammation and are considered to be crucial contributors in development of cardiovascular diseases. In *in vivo* studies, the elevated VCAM-1 and ICAM-1 expression levels in endothelial cells were detected within regions predisposed to atherosclerotic lesion formation (Endres, Laufs, Merz, & Kaps, 1997; O'Brien et al., 1996). For this reason, an increasing interest has been focused on investigations of compounds against the over-expression of adhesion molecules in endothelial cells. So far, some anti-inflammatory agents such as paeonol, cinnamaldehyde and epigallocatechin have been known to diminish the expression of VCAM-1 and ICAM-1 in HUVECs (Chae et al., 2007; Liao et al., 2008; Nizamutdinova et al., 2007). As for COS, previous studies confirmed their inhibitory effects on inflammatory responses (Dou et al., 2007; Wu & Tsai, 2007; Yoon et al., 2007), implying the potential roles in improving endothelial dysfunction associated with over-expressed pro-inflammatory cytokines. In this study, we for the first time demonstrated that COS could inhibit the production of VCAM-1 and ICAM-1 in TNF-α-induced HUVECs through p38 MAPK and ERK1/2 pathways.

In the vascular inflammation, adhesion molecules are mainly regulated by pro-inflammatory stimuli and several types of inflammatory cytokines have been reported to induce the production of VCAM-1 and ICAM-1. It was reported that TNF-α induced inflammatory responses by enhancing ICAM-1 surface expression in HUVECs (Nizamutdinova et al., 2007). Chae et al. (2007) proved that angiotensin-II led to the elevation of membrane-associated VCAM-1 and ICAM-1 production in HUVECs. Additionally, LPS was also found to induce VCAM-1 and ICAM-1 expression in human aortic vascular smooth muscle cells (Heo, Yun, Noh, Park, & Park, 2008). These reports are consistent with our findings that activation of HUVECs with TNF-α (20 ng/ml) resulted in an up-regulated expression of VCAM-1 and ICAM-1. Moreover, the TNF-α-induced over-expression of both adhesion molecules was ameliorated by pretreatment with COS (50–200 μg/ml) for 24 h, indicating that COS can act as an inhibitor of TNF-α-induced VCAM-1 and ICAM-1 expression in HUVECs. Since no significant growth inhibition of HUVECs was observed after exposed to COS alone (50–200 μg/ml) for 24 h, the inhibitory effects of COS on production of both adhesion molecules appeared not to be the cytotoxic activities. Other evidence in support of this view is from our adhesion analysis of U937 monocytes to activated HUVECs showing that pretreatment with COS (50–200 μg/ml) for 24 h obviously attenuated TNF-α-induced U937 monocyte adhesion. These results presented here not only imply that COS may protect endothelial cells against TNF-α-induced damage but also partly explain why COS have suppressive effects on endothelial dysfunction.

NF-κB is a transcription factor that commonly resides in the cytoplasm of unstimulated cells by binding to its inhibitory protein IκB (Kim et al., 2008). When stimulated by extracellular signals, IκB is phosphorylated and rapidly degraded through proteolysis, allowing the release of NF-κB and subsequent translocation into the nucleus to activate its target genes (Ponce et al., 2009). It has been well established that activation of NF-κB by TNF-α leads to over-production of inflammatory adhesion molecules such as VCAM-1 and ICAM-1 (Oesterling et al., 2008). In this study, we demonstrated that TNF-α-induced NF-κB activation and IκBα degradation was inhibited by COS (50–200 μg/ml). This finding is in accordance with a recent study which showed that interferon-γ-induced activation of NF-κB in RAW264.7 macrophages was inhibited by a low-molecular weight chitosan (20 kDa) (Wu & Tsai, 2007). Additionally, previous studies also revealed that the inhibition of NF-κB completely blocked TNF-α-induced expression of VCAM-1 and ICAM-1 (Rajan, Ye, Bai, Huang, & Guo, 2008). Together, these results suggest that suppressive effects of COS on the gene expression of VCAM-1 and ICAM-1 are at least in part due to its inhibition against NF-κB activation.

There are some studies suggesting that MAPKs are positively related to TNF-α signaling in HUVECs (Chai, Wang, Huang, Xie, & Fu, 2008; Sun et al., 2008; Vietor et al., 1993). Further, the results from Nizamutdinova et al. (2007), Nizamutdinova et al. (2008) indicate that p38 MAPK and ERK1/2, but not c-Jun N-terminal kinase (JNK), are involved in TNF-α-induced protein production of VCAM-1 and ICAM-1. We, therefore, focused the rest of our studies on p38 MAPK and ERK1/2. We found that induction of HUVECs by TNF-α increased the levels of p-p38 MAPK and p-ERK1/2, suggesting the critical roles of both MAPKs in TNF-α-activated signal transduction pathways. On the other hand, the COS pretreatment not only attenuated TNF-α-induced p38 MAPK phosphorylation from 50 to 200 μg/ml, but also suppressed ERK1/2 phosphorylation at 100 μg/ml. Collectively, the effects of COS on HUVECs may be

attributed to the inhibition of phosphorylated levels of both MAPKs.

MAPKs are known to be involved in the NF-κB activation in murine RAW264.7 macrophages (Aga et al., 2004). Regretfully, no studies were reported that p38 MAPK and ERK1/2 phosphorylation were required for TNF-α-induced NF-κB activation in HUVECs. To address this, we performed experiments by using selective kinase inhibitors, SB203580 (25 μM) against p38 MAPK and PD98059 (25 μM) against ERK1/2, confirmed that the levels of p-p38 MAPK and p-ERK1/2 were positively associated with NF-κB activation in TNF-α-induced HUVECs. This observation suggests that inhibitory effects of COS on NF-κB activation might be regulated via the p38 MAPK and ERK1/2-dependent pathways. Also, SB203580 and PD98059 suppressed TNF-α-induced VCAM-1 and ICAM-1 mRNA expression in HUVECs. As a result, we propose that up-regulation of p38 MAPK and ERK1/2 phosphorylation induced by TNF-α initiates the translocation of NF-κB into nucleus and then triggered the over-expression of VCAM-1 and ICAM-1. From these studies, it may be concluded that COS can inhibit TNF-α-induced elevation of VCAM-1 and ICAM-1 levels in HUVECs through the inhibition of p38 MAPK and ERK1/2 signaling pathways resulting in an activation of NF-κB.

Noticeably, the inhibition of VCAM-1 and ICAM-1 production by COS in TNF-α-induced HUVECs seemed not to depend on the drug concentration. COS at 100 μg/ml displayed a better inhibition than other two concentrations (50 and 200 μg/ml). In previous studies, we have shown that the inhibitory effects of COS on hydrogen peroxide-induced stress injury in HUVECs were not strictly dose-dependent (Liu et al., 2009). In addition, our findings are just phenomenological and we failed to find the target molecules of COS triggering MAPK pathways in HUVECs. These results indicate that the action of COS may be complex and further efforts are required to elucidate underlying mechanisms by which COS exerts the best biological effects.

In conclusion, this study demonstrated that COS potently inhibited the expression of VCAM-1 and ICAM-1 in HUVECs induced by TNF-α at the level of transcription and translation. Moreover, COS suppressed TNF-α-induced activation of NF-κB, degradation of IκBα, and phosphorylation of p38 MAPK and ERK1/2 in HUVECs. These results provided direct evidence on the protective effects of COS against endothelial dysfunction, and our findings may suggest a novel application for COS in treatment of vascular inflammation, in particular diseases involving adhesion molecules.

Acknowledgments

This work was supported by National Programs for High Technology Research and Development (863 Programs, 2006AA100313 and 2007AA10Z343), and by Natural Science Fund of Chong Qing, China (KJ070304).

References

Aga, M., Watters, J. J., Pfeiffer, Z. A., Wiepz, G. J., Sommer, J. A., & Bertics, P. J. (2004). Evidence for nucleotide receptor modulation of cross talk between MAP kinase and NF-kappa B signaling pathways in murine RAW 264.7 macrophages. *American Journal of Physiology Cell Physiology, 286*, C923–C930.

Chae, Y. J., Kim, C. H., Ha, T. S., Hescheler, J., Ahn, H. Y., & Sachinidis, A. (2007). Epigallocatechin-3-O-gallate inhibits the angiotensin II-induced adhesion molecule expression in human umbilical vein endothelial cell via inhibition of MAPK pathways. *Cellular Physiology and Biochemistry, 20*, 859–866.

Chai, H., Wang, Q., Huang, L., Xie, T., & Fu, Y. (2008). Ginsenoside Rb1 inhibits tumor necrosis factor-alpha-induced vascular cell adhesion molecule-1 expression in human endothelial cells. *Biological & Pharmaceutical Bulletin, 31*, 2050–2056.

Cianchetti, S., Del Fiorentino, A., Colognato, R., Di Stefano, R., Franzoni, F., & Pedrinelli, R. (2008). Anti-inflammatory and anti-oxidant properties of telmisartan in cultured human umbilical vein endothelial cells. *Atherosclerosis, 198*, 22–28.

Dou, J. L., Tan, C. Y., Du, Y. G., Bai, X. F., Wang, K. Y., & Ma, X. J. (2007). Effects of chitooligosaccharides on rabbit neutrophils in vitro. *Carbohydrate Polymers, 69*(2), 209–213.

Endres, M., Laufs, U., Merz, H., & Kaps, M. (1997). Focal expression of intercellular adhesion molecule-1 in the human carotid bifurcation. *Stroke, 28*, 77–82.

Haubner, F., Lehle, K., Münzel, D., Schmid, C., Birnbaum, D. E., & Preuner, J. G. (2007). Hyperglycemia increases the levels of vascular cellular adhesion molecule-1 and monocyte-chemoattractant-protein-1 in the diabetic endothelial cell. *Biochemical and Biophysical Research Communications, 360*, 560–565.

Heo, S. K., Yun, H. J., Noh, E. K., Park, W. H., & Park, S. D. (2008). LPS induces inflammatory responses in human aortic vascular smooth muscle cells via Toll-like receptor 4 expression and nitric oxide production. *Immunology Letters, 120*, 57–64.

Je, J. Y., Park, P. J., & Kim, S. K. (2004). Free radical scavenging properties of hetero-chitooligosaccharides using an ESR spectroscopy. *Food and Chemical Toxicology, 42*, 381–387.

Kim, S. R., Bae, Y. H., Bae, S. K., Choi, K. S., Yoon, K. H., Koo, T. H., et al. (2008). Visfatin enhances ICAM-1 and VCAM-1 expression through ROS-dependent NF-kappaB activation in endothelial cells. *Biochimica Biophysica Acta, 1783*, 886–895.

Liao, B. C., Hsieh, C. W., Liu, Y. C., Tzeng, T. T., Sun, Y. W., & Wung, B. S. (2008). Cinnamaldehyde inhibits the tumor necrosis factor-alpha-induced expression of cell adhesion molecules in endothelial cells by suppressing NF-kappaB activation: effects upon IkappaB and Nrf2. *Toxicology and Applied Pharmacology, 229*, 161–171.

Lidington, E. A., Moyes, D. L., McCormack, A. M., & Rose, M. L. (1999). A comparison of primary endothelial cells and endothelial cell lines for studies of immune interactions. *Transplant Immunology, 7*, 239–246.

Liu, H. T., Li, W. M., Xu, G., Li, X. Y., Bai, X. F., Wei, P., et al. (2009). Chitosan oligosaccharides attenuate hydrogen peroxide-induced stress injury in human umbilical vein endothelial cells. *Pharmacological Research, 59*, 167–175.

Mendis, E., Kim, M. M., Rajapakse, N., & Kim, S. K. (2007). An in vitro cellular analysis of the radical scavenging efficacy of chitooligosaccharides. *Life Sciences, 80*, 2118–2127.

Moon, J. S., Kim, H. K., Koo, H. C., Joo, Y. S., Nam, H. M., Park, Y. H., et al. (2007). The antibacterial and immunostimulative effect of chitosan-oligosaccharides against infection by *Staphylococcus aureus* isolated from bovine mastitis. *Applied Microbiology and Biotechnology, 75*, 989–998.

Nizamutdinova, I. T., Jeong, J. J., Xu, G. H., Lee, S. H., Kang, S. S., Kim, Y. S., et al. (2008). Hesperidin, hesperidin methyl chalone and phellopterin from *Poncirus trifoliata* (Rutaceae) differentially regulate the expression of adhesion molecules in tumor necrosis factor-alpha-stimulated human umbilical vein endothelial cells. *International Immunopharmacology, 8*, 670–678.

Nizamutdinova, I. T., Oh, H. M., Min, Y. N., Park, S. H., Lee, M. J., Kim, J. S., et al. (2007). Paeonol suppresses intercellular adhesion molecule-1 expression in tumor necrosis factor-alpha-stimulated human umbilical vein endothelial cells by blocking p38, ERK and nuclear factor-kappaB signaling pathways. *International Immunopharmacology, 7*, 343–350.

O'Brien, K. D., McDonald, T. O., Chait, A., Allen, M. D., & Alpers, C. E. (1996). Neovascular expression of E-selectin, intercellular adhesion molecule-1, and vascular cell adhesion molecule-1 in human atherosclerosis and their relation to intimal leukocyte content. *Circulation, 93*, 672–682.

Oesterling, E., Chopra, N., Gavalas, V., Arzuaga, X., Lim, E. J., Sultana, R., et al. (2008). Alumina nanoparticles induce expression of endothelial cell adhesion molecules. *Toxicology Letters, 178*, 160–166.

Pae, H. O., Seo, W. G., Kim, N. Y., Oh, G. S., Kim, G. E., Kim, Y. H., et al. (2001). Induction of granulocytic differentiation in acute promyelocytic leukemia cells (HL-60) by water-soluble chitosan oligomer. *Leukemia Research, 25*, 339–346.

Ponce, C., Torres, M., Galleguillos, C., Sovino, H., Boric, M. A., Fuentes, A., et al. (2009). Nuclear factor kappaB pathway and interleukin-6 are affected in eutopic endometrium of women with endometriosis. *Reproduction, 137*, 727–737.

Rajan, S., Ye, J., Bai, S., Huang, F., & Guo, Y. L. (2008). NF-kappaB, but not p38 MAP kinase, is required for TNF-alpha-induced expression of cell adhesion molecules in endothelial cells. *Journal of Cellular Biochemistry, 105*, 477–486.

Séguin, C., Abid, M. R., Spokes, K. C., Schoots, I. G., Brkovic, A., Sirois, M. G., et al. (2008). Priming effect of homocysteine on inducible vascular cell adhesion molecule-1 expression in endothelial cells. *Biomedicine & Pharmacotherapy, 62*, 395–400.

Sun, D. I., Nizamutdinova, I. T., Kim, Y. M., Cai, X. F., Lee, J. J., Kang, S. S., et al. (2008). Bisacurone inhibits adhesion of inflammatory monocytes or cancer cells to endothelial cells through down-regulation of VCAM-1 expression. *International Immunopharmacology, 8*, 1272–1281.

Vietor, I., Schwenger, P., Li, W., Schlessinger, J., & Vilcek, J. (1993). Tumor necrosis factor-induced activation and increased tyrosine phosphorylation of mitogen-activated protein (MAP) kinase in human fibroblasts. *Journal of Biological Chemistry, 268*, 18994–18999.

Winterbone, M. S., Tribolo, S., Needs, P. W., Kroon, P. A., & Hughes, D. A. (2009). Physiologically relevant metabolites of quercetin have no effect on adhesion molecule or chemokine expression in human vascular smooth muscle cells. *Atherosclerosis, 202*, 431–438.

Wu, G. J., & Tsai, G. J. (2007). Chitooligosaccharides in combination with interferon-gamma increase nitric oxide production via nuclear factor-kappaB activation in murine RAW264.7 macrophages. *Food and Chemical Toxicology, 45*, 250–258.

Yan, Y., Wanshun, L., Baoqin, H., Bing, L., & Chenwei, F. (2006). Protective effects of chitosan oligosaccharide and its derivatives against carbon tetrachloride-induced liver damage in mice. *Hepatology Research, 35*, 178–184.

Yoon, H. J., Moon, M. E., Park, H. S., Im, S. Y., & Kim, Y. H. (2007). Chitosan oligosaccharide (COS) inhibits LPS-induced inflammatory effects in RAW 264.7 macrophage cells. *Biochemical and Biophysical Research Communications, 358*, 954–959.

Yoon, H. J., Moon, M. E., Park, H. S., Kim, H. W., Im, S. Y., Lee, J. H., et al. (2008). Effects of chitosan oligosaccharide (COS) on the glycerol-induced acute renal failure in vitro and in vivo. *Food and Chemical Toxicology, 46*, 710–716.

Zhang, H., Du, Y. G., Yu, X., Mitsutomi, M., & Aiba, S. (1999). Preparation of chitooligosaccharides from chitosan by a complex enzyme. *Carbohydrate Research, 320*, 257–260.

Zhou, Z., Liu, Y., Miao, A. D., & Wang, S. Q. (2005). Protocatechuic aldehyde suppresses TNF-alpha-induced ICAM-1 and VCAM-1 expression in human umbilical vein endothelial cells. *European Journal of Pharmacology, 513*, 1–8.